

# Stability Analyses of Visual-lifting Biped Walking Based on Feedforward and Feedback Calculation

Keli Shen, Xiang Li, Hongzhi Tian, Daiji Izawa and Mamoru Minami

**Abstract**—The fields of robotics and control are making effort to develop biped robots that can realize walking motions with the stability and flexibility like humans'. Dynamic walking models of biped robots are hybrid in nature. In previous study, biped walking control has been realized by Zero-Moment Point (ZMP). The efficiency of ZMP was well verified in keeping stable walking, but ZMP based walking cannot stop falling down when the gait is tiptoe state. Besides, dynamical walking can be used for walking that realizes kicks by toes, which does not depend on ZMP. Though the dynamical walking seems to be natural, robots tend to fall down. Therefore, it is necessary to keep the stability of dynamical walking. In our study, we have proposed a dynamical equation for walking derived by the Newton-Euler method including slipping, impact, point-touchdown and surface-touchdown of the foot. "Visual Lifting Approach" (VLA) can enhance the stability of standing and walking and prevents bipeds from falling without using ZMP. The combined control includes visual-lifting feedback and swinging feedforward, which can realize the switch of walking gaits. In this paper, we analyze the realization of the stable walking according to some dynamical measurements.

## I. INTRODUCTION

In many biped-walking control strategies of the humanoid, ZMP-based walking motion is considered as most efficient method, which has been certified to be useful in keeping stability of practical biped-walking, since it can make sure that humanoid robots can keep the balance of walking and standing by retaining the ZMP within the convex hull of supporting area [1], [2]. However, ZMP control makes the humanoid robot's waist lower and robot's walking looks like monkey's. Besides, other methods except ZMP has been proposed to concentrate on keeping the biped-walking trajectories in side of a basin of attraction [3], [4], [5], including a way referring limit cycle to determine input torques [6].

These previous methods discussed are based on simplified biped models, which try to avoid discussing the effects of feet or slipping existing in real environment. Different from the above reference, one study [7] has pointed out the effect of foot having many walking gaits such as surface contacting (foot sole contacting with ground) and point contacting (heel contacting), changing the dimension of state variables. Our research has started from view point of [7] to describe the dynamics of gaits including point/surface-contacting state, slipping and bumping of foot as correctly as possible. It is called event-driven where walking gait transition would be

determined by the past walking motion. The model in [7] only has foot model different from our model including the dynamics of whole-body humanoid with arms and head. And what the authors want to point out is that the dimensions of equations of motion are changed by the varieties of the biped-walking introduced in [8] concerning one-legged hopping robot.

Further the tipping over motion has been called non-holonomic dynamics including a joint such as free joint without inputting torque. At the same time, the heel or the toe of lifting foot in the air contacts with the ground geometrically. The referred paper [9] discussed the method of representing contacting with environment dealing constraint motion with friction by algebraic equation and applied it to human configuration [10]. According to these references, dynamics of 21 kinds of gaits were derived including slipping motion with both different constraint conditions and change of the dimension of state variables where the humanoid's dynamical model has been sufficiently denoted as much as possible [11].

In previous research on VLA in [12], [13], the incomplete model of humanoid was applied in which head, arms and torso were neglected. Thus, there are some drawbacks, i.e., the model was too simple to consider the effect of dynamical coupling of arm and upper body. However, the new model proposed in this paper has been optimized concerning the above problem, and the discussion of slipping and effectiveness of the model have been proved in [11].

Visual-lifting Approach(VLA) based on visual servoing has been proposed which can realize the natural walking with slippage including toe-off state. Real-time position and orientation tracking method to observe a 3D object that is put near the humanoid to measure the robot's head relative pose has been proposed as visual pose estimation [14]. And added feedforward inputs are used to keep the leg joints rotating for walking. The simulation results indicate that visual feedback control and swinging feedforward inputs are useful to realize the stable biped-walking on the condition that humanoid's dynamics includes toe-off, slipping and bumping. Besides, this paper analyzes the stability of walking according to some dynamical measurements.

## II. DYNAMICAL BIPED WALKING MODEL

The biped-walking robot in Fig. 1 is discussed in this paper, Table I shows length  $l_i$  [m], mass  $m_i$  [kg] of links and coefficient of joints' viscous friction  $d_i$  [N·m·s/rad], which are determined by [15]. This model is simulated as a serial-link manipulator having branches and represents rigid whole-

K. Shen, X. Li, H. Zhi, D. Izawa and M. Minami are with Graduate School of Natural Science and Technology, Okayama University, Okayama, Japan 700-8530 {pue85qr6, pzkm87r2, psnc8ytd}@s.okayama-u.ac.jp, {minami-m}@cc.okayama-u.ac.jp

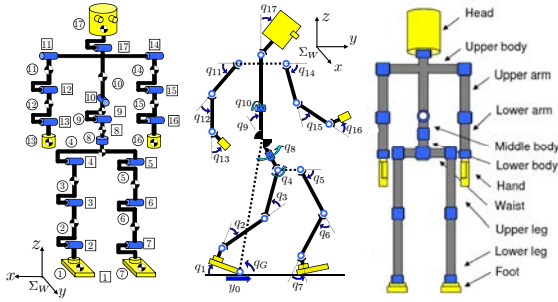


Fig. 1. Definition of biped-walking model, ①~⑰ represents link number, 1~17 is joint number,  $q_1 \sim q_{17}$  is joint angles.

TABLE I

PHYSICAL PARAMETERS

Link	$l_i$ [m]	$m_i$ [kg]	$d_i$ [Nms/rad]
Head	0.24	4.5	0.5
Upper body	0.41	21.5	10.0
Middle body	0.1	2.0	10.0
Lower body	0.1	2.0	10.0
Upper arm	0.31	2.3	0.03
Lower arm	0.24	1.4	1.0
Hand	0.18	0.4	2.0
Waist	0.27	2.0	10.0
Upper leg	0.38	7.3	10.0
Lower leg	0.40	3.4	10.0
Foot	0.07	1.3	10.0
Total weight [kg]	—	64.2	—
Total height [m]	1.7	—	—

body such as feet including toe, torso, arms and so on and is up to 17 degree-of-freedom (DOFs). Though motion of legs is limited in sagittal plane, it generates many walking gaits since the robot has flat-sole feet and kicking torque. In this paper, the foot named as link-1 is defined as “supporting-foot” and the other foot named as link-7 is defined as “free foot” (“contacting-foot” when the floating foot contacts with ground) according to gaits. When the contacting-foot stops slipping which indicates that static friction force is exerted on the foot, the contacting-foot switches to supporting-foot and the previous supporting-foot is transferred into free foot if it was isolated from floor.

### III. DYNAMICAL CALCULATION AND ANALYSES

Equation of motion with one foot standing can be obtained,

$$M(\mathbf{q})\ddot{\mathbf{q}} + \mathbf{h}(\mathbf{q}, \dot{\mathbf{q}}) + \mathbf{g}(\mathbf{q}) + \mathbf{D}\dot{\mathbf{q}} = \boldsymbol{\tau}, \quad (1)$$

Here,  $\boldsymbol{\tau} = [f_{y_0}, \tau_1, \tau_2, \dots, \tau_{17}]$  is input torque, where  $f_{y_0}$  is always zero since the slipping motion has no actuators.  $M(\mathbf{q})$  is inertia matrix,  $\mathbf{h}(\mathbf{q}, \dot{\mathbf{q}})$  is the vector indicating Coriolis force and centrifugal one, and  $\mathbf{g}(\mathbf{q})$  is gravity one. The  $\mu_k$  in  $\mathbf{D} = \text{diag}[\mu_k, d_1, d_2, \dots, d_{17}]$  represents coefficient of friction,  $\mu_k$  is the one between foot and ground. And  $\mathbf{q} = [y_0, q_1, q_2, \dots, q_{17}]^T$  includes the relative position

between foot and ground  $y_0$  generated by slipping and the angle of joints  $q_1 \sim q_{17}$ .

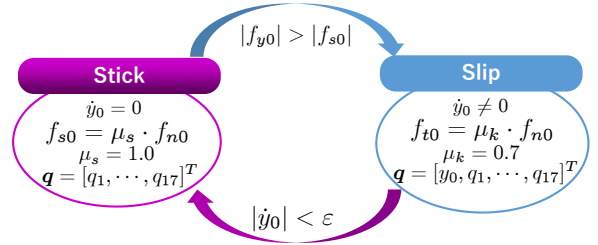


Fig. 2. Switch conditions of stick-slip motion during the walking

This stick motion state is described at left side of Fig. 2. If  $|\dot{y}_0| < \epsilon$  is satisfied, the degree of motion  $y_0$  will disappear and the equation of motion will transfer to the equation of motion consisting of  $\mathbf{q} = [q_1, q_2, \dots, q_{17}]^T$ . On this state, static friction coefficient  $\mu_s = 1.0$  is employed, and static friction force  $f_{s0} = \mu_s f_{n0}$  exerts to the lateral direction of foot.

However, when the supporting-foot (1-st link) is slipping (prismatic joint is added), the force exerting onto the 1-st link can be calculated by following equation.

$$f_{y_0} = \mathbf{e}_{z_0}^T \mathbf{f}_0 + \mu_k \dot{y}_0. \quad (2)$$

where  $\dot{y}_0$  is velocity of slippage. The viscous friction force along  $y$ -axis (slipping axis) described as  $\mu_k \dot{y}_0$  is shown in right-hand side of Eq. (2).

If the exerting lateral force  $f_{y_0}$  generated by dynamical coupling of humanoid body calculated by Eq. (2) satisfies  $|f_{y_0}| > |f_{s0}|$ , the slipping motion will start and the equation of motion, Eq. (2), will be changed into the one with variables of  $\mathbf{q} = [y_0, q_1, q_2, \dots, q_{17}]^T$  again, which is shown at the right state Fig. 2.

### IV. COMBINED BIPED WALKING CONTROL METHOD

1) VISUAL LIFTING APPROACH FOR KEEPING STANDING AND WALKING: Visual Lifting Approach has been proposed, which can improve the stability of biped standing and walking as shown in Fig.3. We apply a model-based matching method to measure the posture of a static target object described by  $\boldsymbol{\psi}(t) = [X_{head}(t), Y_{head}(t), Z_{head}(t), \phi_{head}(t), \theta_{head}(t), \psi_{head}(t)]$  representing the position and orientation of robot's head based on  $\Sigma_H$ . The relatively desired head posture coordinate of  $\Sigma_R$  (coordinate of reference target object) and the current head posture coordinate  $\Sigma_H$  are predefined by Homogeneous Transformation as  ${}^H T_R$ . The difference between the desired head posture coordinate  $\Sigma_{H_d}$  and the current head posture coordinate  $\Sigma_H$  is defined as  ${}^H T_{H_d}$ , it can be described by:

$${}^H T_{H_d}(\boldsymbol{\psi}_d(t), \boldsymbol{\psi}(t)) = {}^H T_R(\boldsymbol{\psi}(t)) \cdot {}^{H_d} T_R^{-1}(\boldsymbol{\psi}_d(t)), \quad (3)$$

where  ${}^H T_R$  is calculated by  $\boldsymbol{\psi}(t)$ .  $\boldsymbol{\psi}(t)$  can be measured by on-line visual posture evaluation proposed by [14]. However,

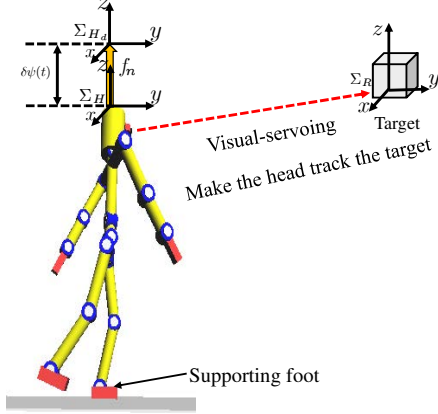


Fig. 3. Concept of Visual Lifting Approach stabilizing walking.

we assume that this parameter is given directly. Here, the force is considered to be directly proportional to  $\delta\psi(t)$ , which is exerted on the head to minimize the deviation  $\delta\psi(t) (= \psi_d(t) - \psi(t))$  calculated from  ${}^H T_{H_d}$ . The deviation of the robot's head posture is caused by gravity force and the influence of walking dynamics. The joint torque  $\tau_h(t)$  lifting the robot's head up and forward is donated:

$$\tau_h(t) = \mathbf{J}_h(\mathbf{q})^T \mathbf{K}_p \delta\psi(t), \quad (4)$$

where  $\mathbf{J}_h(\mathbf{q}) = [\mathbf{J}_{hx}(\mathbf{q}), \mathbf{J}_{hy}(\mathbf{q}), \mathbf{J}_{hz}(\mathbf{q})]^T$  is Jacobian matrix of the head posture against joint angles  $\mathbf{q}$  from supporting foot to head including  $q_1, q_2, q_3, q_4, q_8, q_9, q_{10}, q_{17}$ , and  $\mathbf{K}_p = [20, 290, K_{pz}]$  is lifting proportional gain like impedance control that can adjust joint torque  $\tau_h(t)$  to desired one where  $K_{pz}$  is visual-lifting gain adjusting visual feedback torque inputs along  $z$ -axis direction that can keep the head height targeting the desired one as much as possible and determine that humanoid robots walk like humans or monkeys.  $K_{pz}$  also has special ranges to stabilize the walking. We apply these inputs to stop falling down caused by the influence of gravity or dangerous slipping gaits happening unpredictably during walking progress. We stress that the input torque for non-holonomic joint such as joint-1,  $\tau_{h1}$  in  $\tau_h(t)$  in (4) is zero for its free joint.  $\delta\psi(t)$  can show the deviation of the humanoid's position and orientation, however, only position is discussed in this study.

**2) SWINGING FEEDFORWARD FOR FEET AND BODY'S MOTION:** Besides  $\tau_h(t)$ , in order to make the floating-foot and supporting-foot step forward, input torques  $\tau_t(t) = [0, \tau_{t2}, \tau_{t3}, 0, \tau_{t5}, \tau_{t6}, \tau_{t7}, 0, \dots, 0]^T$  on two legs' joints are added. And another kind of input torques  $\tau_w(t) = [0, \dots, 0, \tau_{w8}, 0, \dots, 0]^T$  added on waist joint is used to swing the roll angle of the waist (joint-8) according to which foot is supporting foot, which further swings two arms with opposite directions by dynamical coupling. Here,  $\tau_t(t)$  and  $\tau_w(t)$  are seen as feedforward input torques. Here,  $t_2$  means the time that supporting-foot and contacting-foot are switched. The elements  $\tau_t(t)$  and  $\tau_w(t)$  are shown below:

$$\tau_{t2} = DA_{t2} \sin(w_{t2}(t - t_2)), \quad (5)$$

$$\tau_{t3} = D[-A_{t3} + A_{t3} \sin(w_{t3}(t - t_2))]. \quad (6)$$

$$\tau_{t5} = \begin{cases} DA_{t51} \cos(w_{t51}(t - t_2)), & (t < 1.0[s]) \\ DA_{t52} \cos(w_{t52}(t - t_2)), & (t \geq 1.0[s]). \end{cases} \quad (7)$$

$$\tau_{t6} = D[-A_{t6} + A_{t6} \sin(w_{t6}(t - t_2))]. \quad (8)$$

$$\tau_{t7} = \begin{cases} DA_{t71}, & (\text{floating}, q_7 \leq 0.6[\text{rad}]) \\ -DA_{t72}, & (\text{contacting}, q_7 \geq 0.35[\text{rad}]) \\ DA_{t73}, & (\text{in other cases}). \end{cases} \quad (9)$$

$$\tau_{w8} = \begin{cases} DA_{w8} \sin(w_{w8}(t - t_2)), & (\text{right foot}) \\ -DA_{w8} \sin(w_{w8}(t - t_2)), & (\text{left foot}). \end{cases} \quad (10)$$

Here,  $D$  is gain of swinging feedforward inputs, amplitudes of torques are set as  $A_{t2} = 10[Nm]$ ,  $A_{t3} = 10[Nm]$ ,  $A_{t51} = 20[Nm]$ ,  $A_{t52} = 15[Nm]$ ,  $A_{t6} = 20[Nm]$ ,  $A_{t71} = 60[Nm]$ ,  $A_{t72} = 40[Nm]$ ,  $A_{t73} = 0[Nm]$ ,  $A_{w8} = 50[Nm]$ . Natural angular frequencies of torques are set as  $w_{t2} = 2\pi[\text{rad/s}]$ ,  $w_{t3} = 2\pi[\text{rad/s}]$ ,  $w_{t51} = 2\pi/1.45[\text{rad/s}]$ ,  $w_{t52} = 2\pi/1.85[\text{rad/s}]$ ,  $w_{t6} = \pi[\text{rad/s}]$ ,  $w_{w8} = 2\pi/1.85[\text{rad/s}]$ .

**3) COMBINED CONTROLLER FOR LIFTING, STEP-PING AND SWINGING:** Combining three kinds of torque inputs in (4)~(10), the controller for biped motion is derived,

$$\tau(t) = \tau_h(t) + \tau_t(t) + \tau_w(t). \quad (11)$$

Here, VLA is applied to keep humanoid robot standing and swinging feedforward is used to make feet step forward.

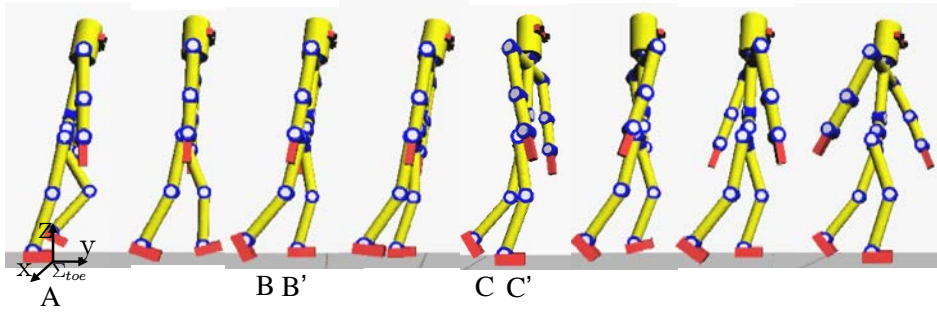
## V. SIMULATION OF BIPED WALKING BASED ON COMPLEXED CONTROL

In the environment that sampling time is set as  $2.0 \times 10^{-4}[s]$  and coefficient of friction between the foot and the ground is set as  $\mu_s = 1.0$  (static friction coefficient),  $\mu_k = 0.7$  (viscous friction coefficient), the walking simulation is finished. The desired position of head is set as  $\psi_d = [0, 0, 2.30[m]]$ .

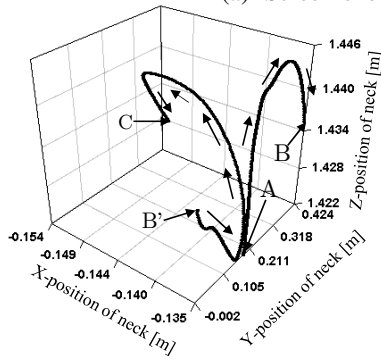
Concerning simulation environment, we used "Borland C++ Builder Professional Ver. 5.0" to make simulation program and "OpenGL Ver. 1.5.0" to display humanoid's time-transient configurations.

In this section, the stability of biped-walking is analyzed according to data obtained in the simulation. In this simulation, we set lifting proportional gain  $\mathbf{K}_p = \text{diag}[20, 290, 1010]$ .

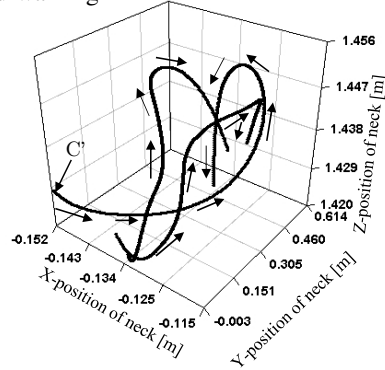
Figure 4 shows the position of the neck during 100-step simulation. The upper part of Fig. 4 shows the screen shot of the biped walking simulation. The point A means the initial posture. B and B' show the state before and after the switching of supporting foot in the 1st step. The points of C and C' show the second time of supporting foot switching. The lower two columns show the transition of position of the



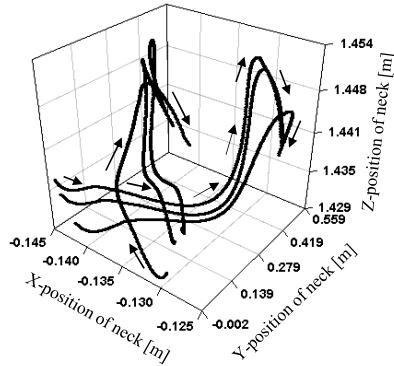
(a) Screen-shot of the biped-walking



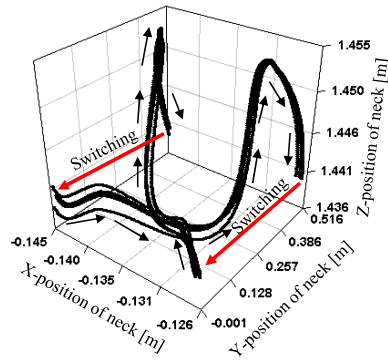
(b) Neck position of 1st~2nd step



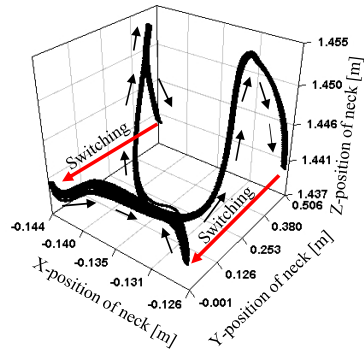
(c) Neck position of 3rd~5th step



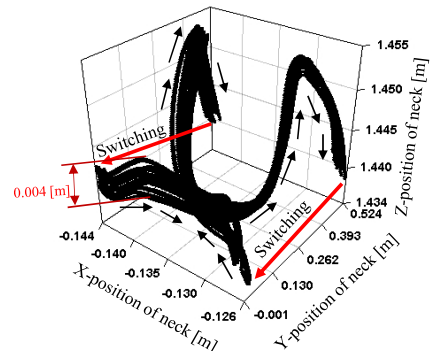
(d) Neck position of 6th~11th step



(e) Neck position of 12th~21st step



(f) Neck position of 22nd~50th step



(g) Neck position of 51st~100th step

Fig. 4. Position of the neck during 100 steps walking simulation. The point of A means the initial posture, B and B' represent the state before and after the switching of supporting-foot in the first step. The C and C' show the second time of supporting foot switching. There are three states in the walking simulation. From 1st step to 5th step is the initial state, and from 6th step to 11th step is the transient state, after 11th step is the stable state.

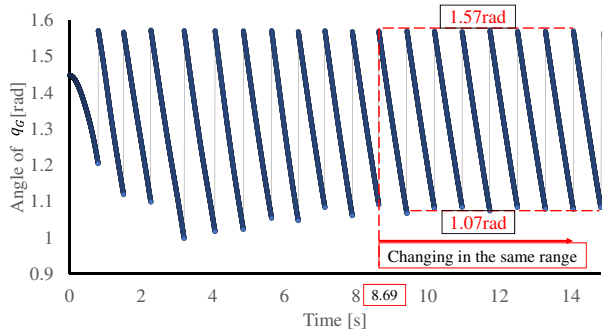


Fig. 5. Angle  $q_G$  between the COG and the origin point of world coordinate system  $\Sigma_w$  which defined in Fig. 1.

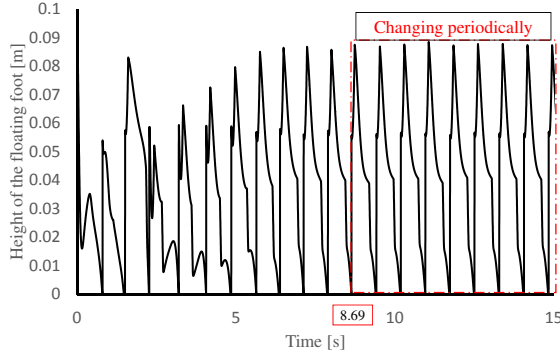


Fig. 6. Height of the floating foot before 15[s].

neck from initial phase and transient phase to stable phase, which are depicted by coordinate  $\Sigma_{toe}$  that is fixed at the toe of the supporting foot. Fig. 4 (b), (c) and (d) shows the initial phase and transient phase, the trajectory is complex and no obvious similarity. In these figures, the position profile with A, B, B', C, C' corresponding to them in screen shots in Fig. 4 (a). After entering stable walking shown in Fig. 4 (e), (f) and (g), the trajectory of the position of the neck is converge to specific tendency, which is similar and along a narrow trajectory ( the width of trajectory is less than  $0.004[m]$ ).

Figure 5 shows the angle  $q_G$  between the COG and the origin of  $\Sigma_{toe}$ . The angle  $q_G$  is defined in Fig. 1, which can illustrate the body's inclination. Before  $8.69[s]$ , the biped robot walks in the initial state and transient state. During these states, the  $q_G$  in each step fluctuates around the different ranges. After  $8.69[s]$ , the  $q_G$  in each step changes in the same range. Figure 5 shows the  $q_G$  changes in the same shape from  $1.57[rad]$  ( about  $90^\circ$  ) to  $1.07[rad]$  ( about  $61.3^\circ$  ) in each step.

Figure 6 and 7 represent the change tendency of height and forward velocity along y-axis of the floating foot before  $15[s]$  respectively. They are also related to the stability of walking. Before  $8.69[s]$ , height and forward velocity change in different forms respectively. After that, they change periodically with the same shape respectively, which means the walking enters the steady state.

In Fig. 8, 9 and 10, X-axis represents the number of step, Y-axis represents the step length, gait cycle and velocity of walking respectively. Biped walking includes three phases: initial phase, transient phase and stable walking phase. From Fig. 8, biped robot walks as the same step length  $0.5[m]$

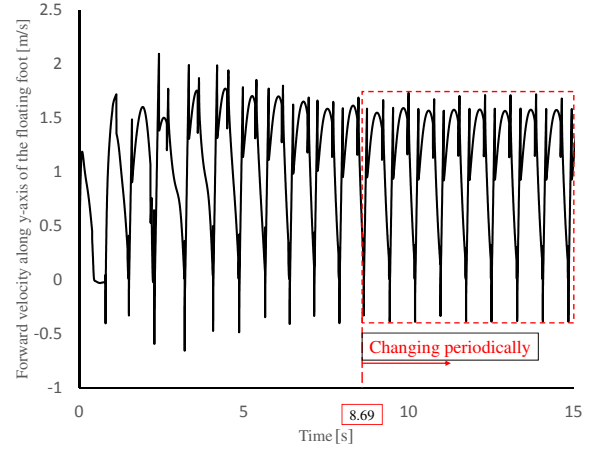


Fig. 7. Forward velocity along y-axis of the floating foot before  $15[s]$ .

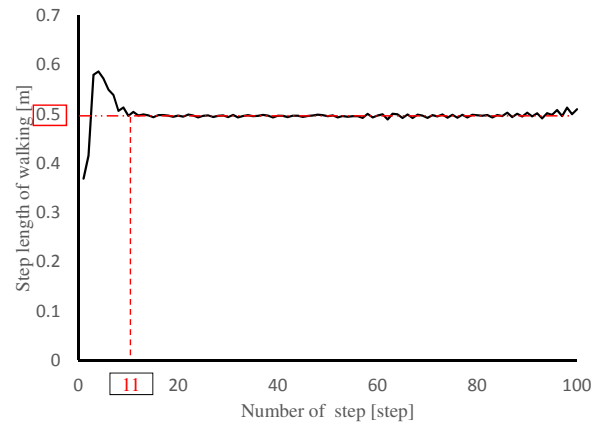


Fig. 8. Step length of biped walking during 100 steps.

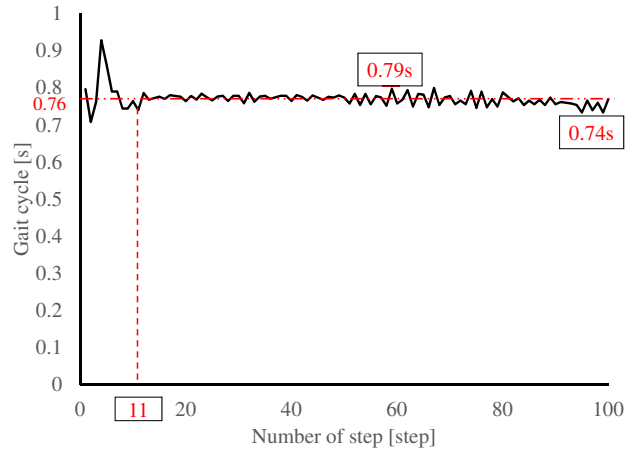


Fig. 9. Gait cycle of biped walking during 100 steps.

after finishing  $11th$  step, which indicates that the biped robot enters the stable walking phase. From Fig. 9, the maximum of gait cycle is  $0.79[s]$  and the minimum of gait cycle is  $0.74[s]$ . The difference value ( $0.05[s]$ ) of gait cycle is very small and most of gait cycle converge to  $0.76[s]$ . In Fig. 10, the maximum of walking velocity is  $2.45[km/h]$  and the minimum of walking velocity is  $2.22[km/h]$ . The average velocity of walking is  $2.34[km/h]$ . Therefore, the velocity of walking changes in a very small range and converge to

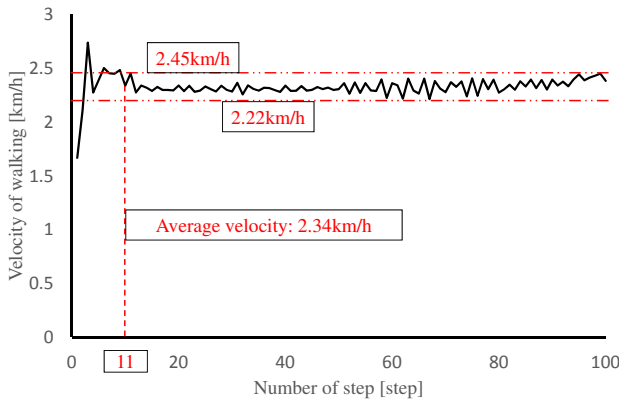


Fig. 10. Velocity of biped walking during 100 steps.

the average velocity. the curve in Fig. 8, 9 and 10 has a divergence trend after its stabilization since biped walking of our model is nonlinear dynamical walking and includes chaos.

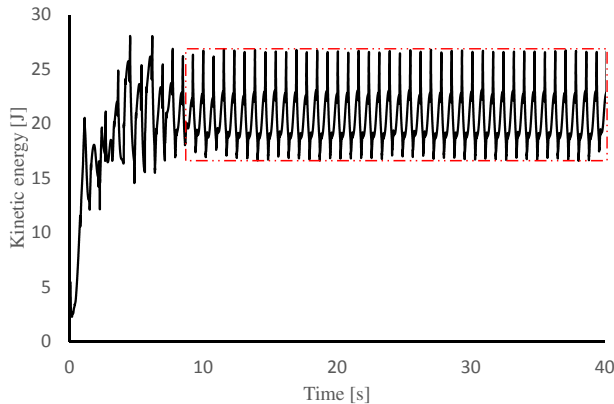


Fig. 11. Kinetic energy of biped walking before 40[s].

Figure 11 and 12 represent the change tendency of the kinematic energy and potential energy before 40[s] respectively. In the initial phase and transient phase, they fluctuate in the large range. After entering the stable walking phase, they change periodically in the same range in each step respectively, which indicates the useful work of the motion is almost same in each step.

## VI. CONCLUSION

In this paper, the stability of walking is proved by some dynamical measurements. The results show visual-lifting feedback control and swinging feedforward inputs based on the dynamical model that contains flat feet including toe, slipping and impact are effective to realize the stable walking, which is human-like natural walking. In the future work, we will adjust visual lifting gains and initial configuration and the height of Center of Gravity to shorten the transient time and increase the stability of walking.

## REFERENCES

[1] M. Vukobratovic, A. Frank and D. Juricic: On the Stability of Biped Locomotion, IEEE Transactions on Biomedical Engineering, Vol.17, No.1 (1970)

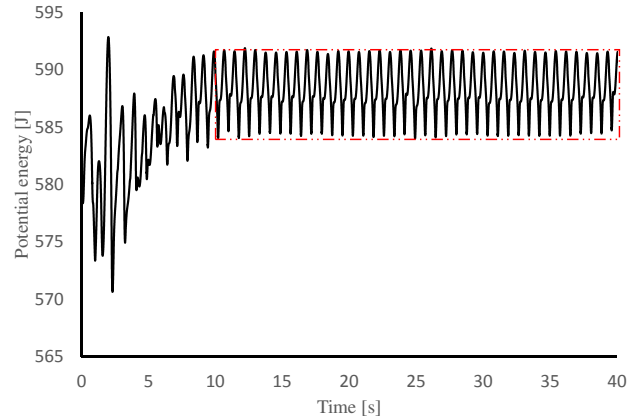


Fig. 12. Potential energy of biped walking before 40[s].

- [2] M. Vukobratovic and J. Stepanenko: On the Stability of Anthropomorphic Systems, *Mathematical Biosciences*, Vol.15 (1972), pp.1-37
- [3] S. Collins, A. Ruina, R. Tedrake and M. Wise: Efficient Bipedal Robots Based on Passive-Dynamic Walkers, *Science*, Vol.307 (2005), pp.1082-1085
- [4] J. Pratt, P. Dilworth and G. Pratt: Virtual Model Control of a Bipedal Walking Robot, *Proceedings of IEEE International Conference on Robotics and Automation*(1997), pp.193-198
- [5] R.E. Westervelt, W.J. Grizzle and E.D. Koditschek: Hybrid Zero Dynamics of Planar Biped Walkers, *IEEE Transactions on Automatic Control*, Vol.48, No.1(2003), pp.42-56
- [6] Y. Harada, J. Takahashi, D. Nenchev and D. Sato: Limit Cycle Based Walk of a Powered 7DOF 3D Biped with Flat Feet, *Proceedings of IEEE/RSJ International Conference on Intelligent Robots and Systems*(2010), pp.3623-3628
- [7] Y. Huang, B. Chen, Q. Wang, K. Wei and L. Wang: Energetic efficiency and stability of dynamic bipedal walking gaits with different step lengths, *Proceedings of IEEE/RSJ International Conference on Intelligent Robots and Systems*(2010), pp.4077-4082
- [8] T. Wu, T. Yeh and B. Hsu: Trajectory Planning of a One-Legged Robot Performing Stable Hop, *Proceedings of IEEE/RSJ International Conference on Intelligent Robots and Systems* (2010), pp.4922-4927
- [9] Y. Nakamura and K. Yamane: Dynamics of Kinematic Chains with Discontinuous Changes of Constraints—Application to Human Figures that Move in Contact with the Environments—, *Journal of RSJ*, Vol.18, No.3(2000), pp.435-443
- [10] K. Yamane and Y. Nakamura: Dynamics Filter - Concept and Implementation of On-Line Motion Generator for Human Figures, *IEEE Transactions on Robotics and Automation*, vol.19, No.3(2003), pp.421-432
- [11] Xiang Li, Hiroki Imanishi, Mamoru Minami, Takayuki Matsuno, Akira Yanou: Dynamical Model of Walking Transition Considering Nonlinear Friction with Floor, *Journal of Advanced Computational Intelligence and Intelligent Informatics*, Vol.20 No.6 (2016)
- [12] Wei Song, Mamoru Minami and Yanan Zhang: A Visual Lifting Approach for Dynamic Bipedal Walking, *International Journal of Advanced Robotic Systems*, Vol.9(2012), pp.1-8
- [13] Akira Yanou, Mamoru Minami, Tomohide Maeba and Yosuke Kobayashi: A First Step of Humanoid's Walking by Two Degree-of-freedom Generalized Predictive Control Combined with Visual Lifting Stabilization, *Proceedings of the 39th Annual Conference of the IEEE Industrial Electronics Society (IECON2013)*, pp.6357-6362
- [14] F. Yu, W. Song and M. Minami: Visual Servoing with Quick Eye-Vergence to Enhance Trackability and Stability, *Proceedings of IEEE/RSJ International Conference on Intelligent Robots and Systems* (2010), pp.6228-6233
- [15] M. Kouchi, M. Mochimaru, H. Iwasawa and S. Mitani: Anthropometric database for Japanese Population 1997-98, *Japanese Industrial Standards Center (AIST, MITI)* (2000)
- [16] T. Maeba, M. Minami, A. Yanou and J. Nishiguchi: Dynamical Analyses of Humanoid's Walking by Visual Lifting Stabilization Based on Event-driven State Transition, *2012 IEEE/ASME Int. Conf. on Advanced Intelligent Mechatronics Proc*(2012), pp.7-14